

Critical rotational speed model of the rotating roll electrode in corona electrostatic separation for recycling waste printed circuit boards

Jia Li, Hongzhou Lu, Zhenming Xu*, Yaohe Zhou

School of Environmental Science and Engineering, Shanghai Jiao Tong University, 800 Dongchuan Road, Shanghai 200240, People's Republic of China

Received 18 August 2007; received in revised form 7 October 2007; accepted 8 October 2007
Available online 13 October 2007

Abstract

Waste printed circuit board (PCB) is increasing worldwide. The corona electrostatic separation (CES) was an effective and environmental protection way to recycle resource from waste PCBs. The aim of this paper is to analyze the main factor (rotational speed) that affects the efficiency of CES from the point of view of electrostatics and mechanics. A quantitative method for analyzing the affection of rotational speed was studied and the model for separating flat nonmetal particles in waste PCBs was established. The conception of “charging critical rotational speed” and “detaching critical rotational speed” were presented. Experiments with the waste PCBs verified the theoretical model, and the experimental results were in good agreement with the theoretical model. The results indicated that the purity and recycle percentage of materials got a good level when the rotational speed was about 70 rpm and the critical rotational speed of small particles was higher than big particles. The model can guide the definition of operator parameter and the design of CES, which are needed for the development of any new application of the electrostatic separation method.

© 2007 Elsevier B.V. All rights reserved.

Keywords: Corona electrostatic separation; Critical rotational speed; Printed circuit board

1. Introduction

The production of printed circuit board (PCB) is increasing worldwide. New technological innovation continues to accelerate the replacement of equipment leading to a significant increase of waste PCBs. Their special physical and chemical characteristic makes that it is difficult to recycle them. In normal PCBs, it can be easily found plenty of toxic materials including heavy metal, PVC plastic, and brominated flame retardants (BFR). However, just like the two-sided coin, the scrap PCBs contain many kinds of metals, which are a rich mine of wealth [1].

The technology of high-voltage has been investigated extensively in the fields of dust precipitation [2,3] and seed sorting [4]. The corona electrostatic separator (CES) was one of the high-voltage technology and has been applied on mineral separation and waste disposal [5–7]. The researchers have successfully used CES to recycle resources from waste PCBs [8].

The structural representation of laboratory CES was shown in Fig. 1. The electric vibratory feeder ensures a monolayer of granular material on the surface of the rotating roll. The high-voltage electrostatic field is generated by corona electrode and electrostatic electrode. The metallic particles lost very fast their charge accrued by ion bombardment, and the charge they carry is that due to electrostatic induction. The electrostatic induction has practically no effect on nonmetal particles, which carry the charge acquired by ion bombardment in the corona discharge and are “pinned” by the electric image force to the rotating roll, and move with it, finally fall in the hold tanks. The electric field forces act differently on the two kind of particles, which achieve the separation goal.

Because the research of corona electrostatic separation involves corona charge, mechanically driven and material property, quantitative and profound theory analysis is good for developing and exploiting this technology. Many researchers have done large quantity of work on electrode arrangement and material humidity [9,10]. But the study about the electrode rotational speed of rotating roll in the process of separating is not thorough enough. The particles charge, separating efficiency and purity are affected by the rotational speed. So, the aim of present

* Corresponding author. Tel.: +86 21 54747495; fax: +86 21 54747495.
E-mail address: zmxu@sjtu.edu.cn (Z. Xu).

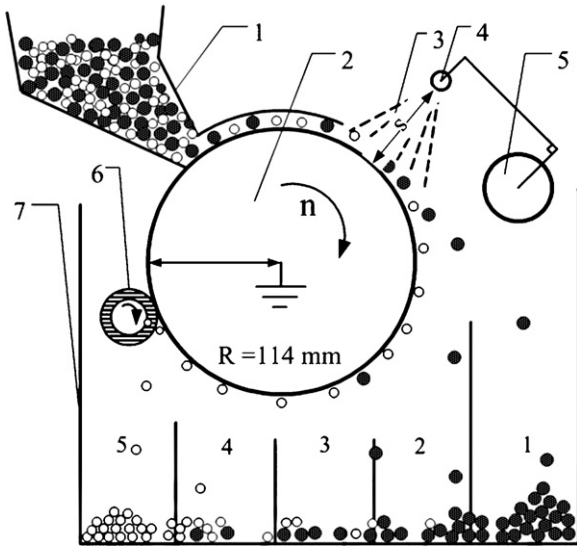


Fig. 1. The structural representation of laboratory roll-type corona electrostatic separator: (1) the feed, (2) the ground roll electrode, (3) the charging field, (4) corona electrode, (5) electrostatic electrode, (6) brush, and (7) holding tanks.

paper is to analyze the impact of rotational speed theoretically and validate the theoretical results through corona electrostatic separating waste PCBs.

2. Theory model

The model is based on the following assumptions: (1) the material was monolayer distributed on the surface of rotating roll and move with it; (2) the distance between two adjacent particles is very big and each particle can be approximated by a material point; and (3) particle interaction was neglected.

As shown in Fig. 1, materials were charged in charging field, during the process of corona electrostatic separation. The corona charge equation was [11]:

$$\frac{dQ}{dt} = \frac{(Q - Q_s)^2}{\tau Q_s} \quad (1)$$

where τ was time delay constant, Q_s was particle's saturated corona charge value. The initial electric charge of particle was:

$$Q(0) = k_Q Q_m \quad (2)$$

where k_Q is a coefficient which depends on field non-uniformity and corona-discharge current ($k_Q \leq 1$) [12]. Because the process of corona charge also includes electrostatic induction charge [13], the induced charge existed. The Q_m was nonmetal particle's maximum induction charge value when the nonmetal particle contacts with rotating roll electrode in the uniform electric field. When the nonmetal particle was sphericity, Q_m was [14]:

$$Q_m = \frac{0.55d^2\pi E\epsilon_0\epsilon_r}{\epsilon_r + 2} \quad (3)$$

where ϵ_0 was vacuum dielectric constant and ϵ_r was particle's dielectric constant. The saturated quantity of corona charge

value of spherical nonmetal particle was calculated [5]:

$$Q_s = \frac{12\pi\epsilon_0r^2E_0\epsilon_r}{\epsilon_r + 2} \quad (4)$$

The whole process of charge includes induction charge, charging neutrality, and corona charge. When nonmetal particle came into the electric field, it was inducted to the positive charge (Q_m). Because the corona electrode was negative electrode, the surface positive charge of particle was neutralized and became negative saturated charge (Q_s). When the particle got 95% of maximum charge value, the delay time was probably five times of charge delay time constant [5].

$$t_s = 5\tau = \frac{20\epsilon_0\epsilon_r}{qk} \quad (5)$$

where q was space charging density, k was ion mobility and $k = 2 \times 10^{-4} \text{ m}^2/(\text{V s})$. The time of nonmetal particle cost in charging field can be computed as follows:

$$t_{gs} = \frac{60e}{2\pi Rn} \quad (6)$$

where e was the width of charging field on the surface of rotating roll electrode, R was the radius of rotating roll electrode, n was the rotational speed of rotating roll electrode. When $t_{gs} > t_s$, particle's charge value reached saturated value, then the rotational speed met:

$$n < n^*, \quad n^* = \frac{3(qke)}{2(\pi\epsilon_0\epsilon_r R)} \quad (7)$$

where n^* was charging critical rotational speed, the charging density q can be computed:

$$q = \frac{J}{Ek} \quad (8)$$

where J was the electric current density on the surface of rotating roll electrode and can be computed:

$$J = \frac{I}{eL} \quad (9)$$

where I was the corona current and L was the length of corona wire. The current–voltage characteristic of corona discharge for different gaps was shown in Fig. 2. Fig. 3 shows the distribution of electric field (without space charges) at the surface of rotating roll electrode which was computed by the software of MATLAB [15]. The research of Jaiswal [16] found that the electric field at the surface of rotating roll electrode with space charge was 2–3 times stronger than the electric field without space charge. In this paper the modified coefficient of electric field was two. The charging rotational speed n^* can be computed from (6)–(9) and Figs. 2 and 3. When discharge gaps $s = 96 \text{ mm}$, applied voltages were 20 kV and 25 kV, the values of n^* were 43.9 rpm and 72.4 rpm separately. If rotational speed was bigger than n^* , the particle could not get saturated quantity of charge, cause the time cost in charging field was too short. Then the Eq. (7) could judge if the particle gets saturated quantity of charge on special rotational speed.

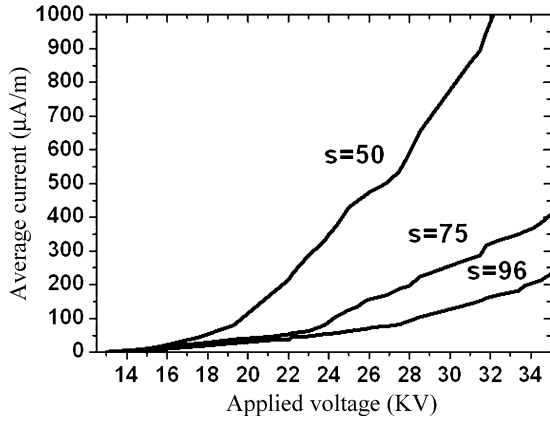


Fig. 2. Current–voltage characteristics of corona discharge for small gaps at negative polarity. (s was the discharge gaps between corona wire and the surface of rotating roll electrode) $R = 114$ mm, corona electrode was wire type, the radius of wire was 0.3 mm.

Most of nonmetal particles were flat, not spherical and the charging value of the particle was correlated with its surface area. The surface equivalent diameter (d_s) was used. The flat particle's d_s was:

$$d_s = \sqrt{\frac{S_p}{\pi}} = \sqrt{r^2 + 2rh} \quad (10)$$

where r was the big surface radius of flat particle and h was the thickness of flat particle. The d_s of flat particle substituted to diameter of spherical in (4). Then the saturated quantity of corona charge value of flat nonmetal particle was:

$$Q_s = \frac{3\pi\epsilon_0(r^2 + 2rh)E_0\epsilon_r}{\epsilon_r + 2} \quad (11)$$

During the process of corona electrostatic separation, the gravitational force (G), centrifugal force (F_w) and image force (F_i) were applying to the nonmetal particle. As shown in Fig. 4, point A was the most probable detaching position from the rotating roll electrode for nonmetal particle. At point A, the particle

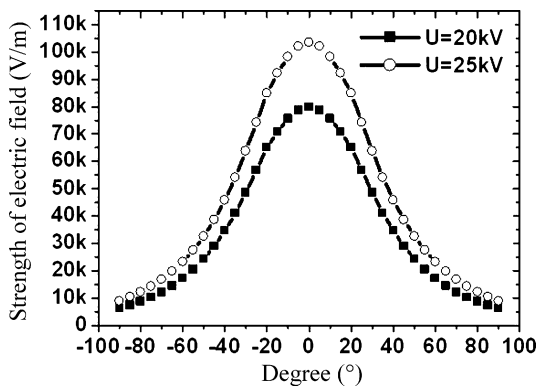


Fig. 3. Distribution of electric field at the surface of rotating roll electrode, for discharge gaps $s = 96$ mm at negative polarity; $R = 114$ mm, corona electrode was wire type, the radius of wire was 0.3 mm; applying the software: Ansys.

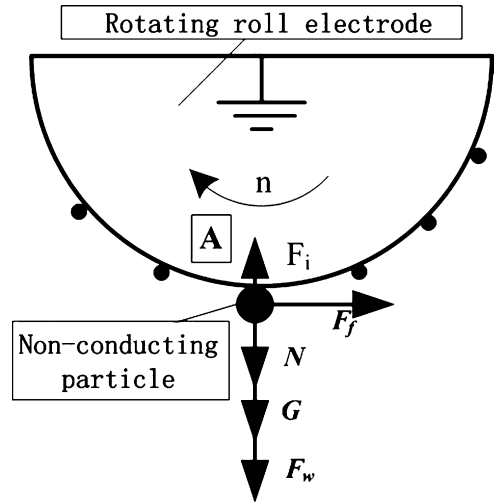


Fig. 4. Force acting on a charged nonmetal particle at the surface of the rotating roll electrode.

was detaching from rotating roll electrode when:

$$F_w + G = F_i \quad (12)$$

It is assumed that the particle gets the saturated quantity of corona charge and with little charge loss. The loss coefficient is named k_1 and it is related to electrical conductivity of particle and rotational speed of rotating roll. In this paper, k_1 is assumed to 0.85, the F_i and F_w can be computed to:

$$F_i = \frac{Q_s^2}{4\pi\epsilon_0 h^2} = BC \quad (13)$$

$$B = \frac{9k_1\pi\epsilon_0\epsilon_r^2 E_0^2}{(\epsilon_r + 2)^2}$$

$$C = \frac{(r^2 + 2rh)^2}{4h^2}$$

$$F_w = m\left(\frac{n\pi}{30}\right)^2 R \quad (14)$$

From (12)–(14), the detaching critical rotational speed of flat nonmetal particle is:

$$n' = \left(\frac{BC}{mR} - \frac{g}{R}\right)^{1/2} \frac{30}{\pi} \quad (15)$$

As shown in Figs. 1 and 4, the critical rotational speed of rotating roll electrode (N) was the speed which ensures the nonmetal particle passes the point A. The situation of nonmetal particle's charge value can be sorted to two kinds.

- (i) $n = n' \leq n^*$, the particle gets the saturated quantity of corona charge value, the N was:

$$N = n' = \left(\frac{BC}{mR} - \frac{g}{R}\right)^{1/2} \frac{30}{\pi} \quad (16)$$

- (ii) $n = n' > n^*$, the particle does not get the saturated quantity of corona charge value, but only $n^*/n' Q_s$. Then from (12)–(16),

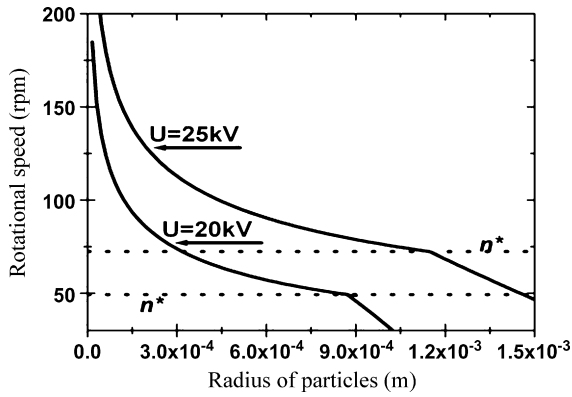


Fig. 5. Calculation relationship curve of critical rotational speed and particle radius.

we have:

$$F'_1 = \frac{Q_s^2}{4\pi\epsilon_0 h^2} \left(\frac{n^*}{n'}\right)^2 = \left(\frac{\pi}{30}\right)^2 \frac{mRBC(n^*)^2}{BC - mg} \quad (17)$$

$$N = \left(\frac{BC(n^*)^2}{BC - mg} - \frac{g}{R} \left(\frac{30}{\pi}\right)^2 \right)^{1/2} \quad (18)$$

From (16) and (18), the N is affected by the particle's radius, the particle's density, the particle's dielectric constant and applied voltage etc. The nonmetal particles were flat particles, the relation of thickness (h) and plan radius (r) was: $h = (1/3)r$. Then from (16) and (18), the relationship of critical rotational speed of rotating roll electrode and particle radius for flat particles was shown in Fig. 5.

3. Materials and experiments

The materials used in this study were scraped waste PCBs [8], as shown in Fig. 6. The mass density of nonmetal particles is 2000 kg/m^3 and the relative dielectric constant of nonmetal particles (ϵ_r) was 3.0. The particle size was $-1.0 + 0.075 \text{ mm}$. The experiments proceed under the different rotational speeds and the applied voltages were 20 kV and 25 kV. As shown in Fig. 1, the No. 1 tank collected metal particles; the No. 5 tank collected nonmetal particles; No. 2–4 tanks collected the mixture of metal and nonmetal particles. The mixture can be separated by the CES again and again to obtain the mass of metal particles and nonmetal particles. The purities of metal particles w_m in No. 1 tank and nonmetal particles w_n in No. 5 tank were measured by the solution quantity with aqua regia [8]. The recycle percentages of metal (r_m) and nonmetal (r_n) particles were:

$$\begin{aligned} r_m &= \frac{Q_1 w_m}{S_m} \\ r_n &= \frac{Q_5 w_n}{S_n} \end{aligned} \quad (19)$$

where Q_1 was the mass of materials in No. 1 tank, Q_5 was the mass of materials in No. 5 tank, S_m was the total mass of metals particles and S_n was the total mass of nonmetal particles.

4. Results and discussion

The separation results of particles with the size of $-0.4 + 0.3 \text{ mm}$ and the applied voltage of 20 kV were shown in Fig. 7. The distribution of nonmetal particles in hold tanks was shown in Fig. 7(a) and the distribution of metal particles in hold tanks was shown in Fig. 7(b). When the rotational speed was 70 rpm, the nonmetal particles in No. 5 hold tank decreased dramatically and the materials in No. 2 hold tank increased.

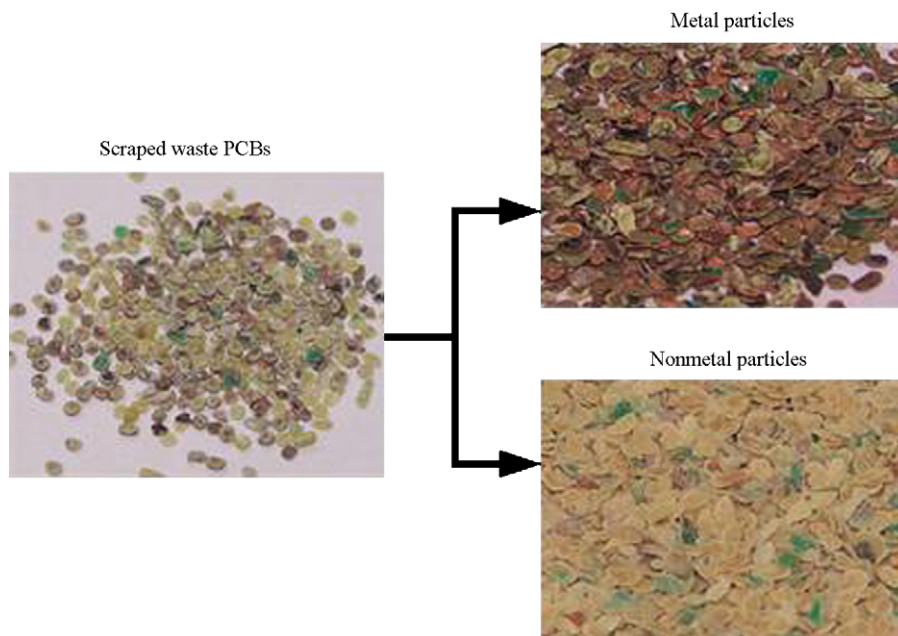


Fig. 6. The scraped waste printed circuit boards.

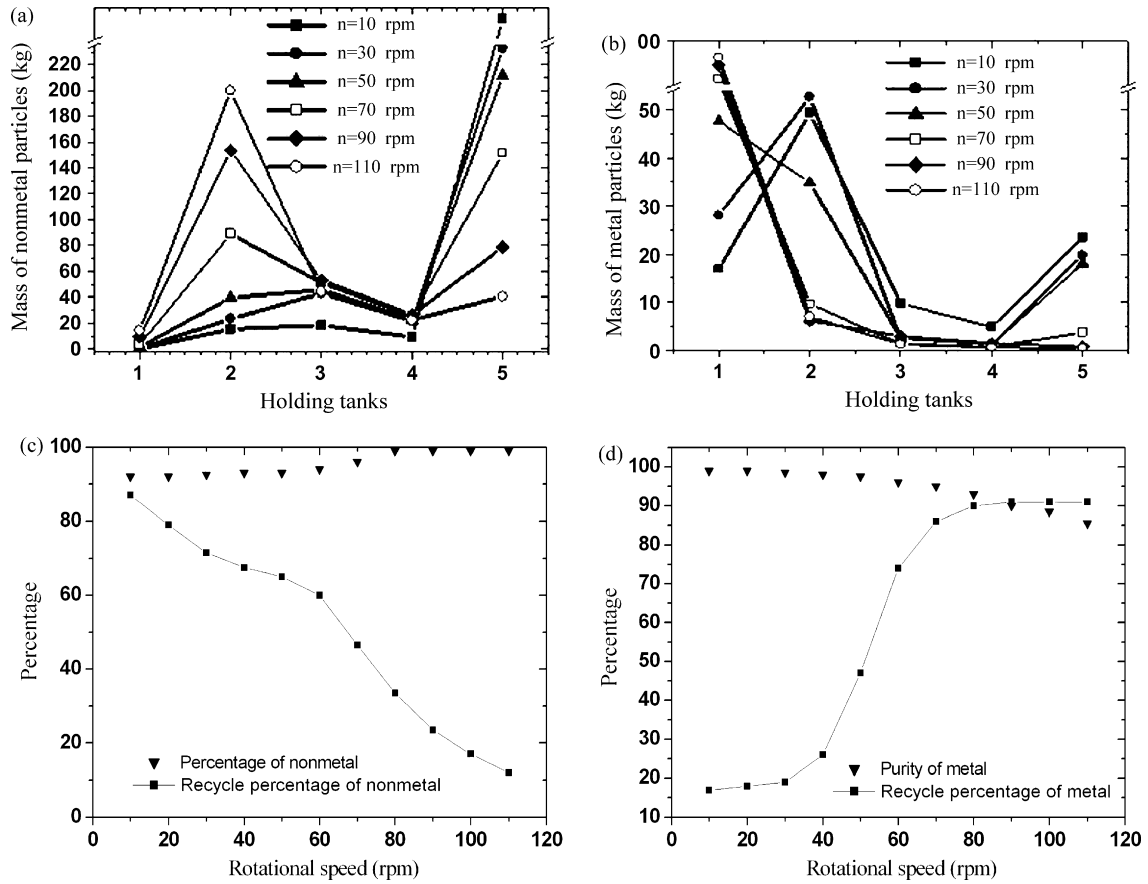


Fig. 7. The separation results for particles $-0.4 + 0.3$ mm: (a) the distribution of nonmetal particles, (b) the distribution of metal particles, (c) purity and recycle percentage of nonmetal particles, and (d) purity and recycle percentage of metal particles.

Fig. 7(c) and (d) showed the purity and recycle percentage of nonmetal particles and metal particles individually under the different rotational speeds. When the rotational speed increased, the recycle percentage of metal particles and the purity of nonmetal particles were increased, but the recycle percentage of nonmetal particles and the purity of metal particles were decreased. As shown in Fig. 7, the purity and recycle percentage of materials got a good level when the rotational speed was about 70 rpm.

The experimental results of critical rotational speed of non-metal particles with the size of $-1.0 + 0.075$ mm were shown in

Fig. 8. The experimental results have a good agreement with the theoretical results. The critical rotational speed of small particles was higher than big particles, as shown in Fig. 8. Because the specific area of small nonmetal particles is big, their relative charging values are high. Increasing the rotational speed can make the metal particles detaching from rotating roll electrode easier. Although the charging value cannot reach the saturated charging value (Q_s), the nonmetal particles can adhere on the surface of rotating roll electrode for their big specific areas. To the big particles, their specific areas are relative small. The charging time and the rotational speed must be limited for the nonmetal

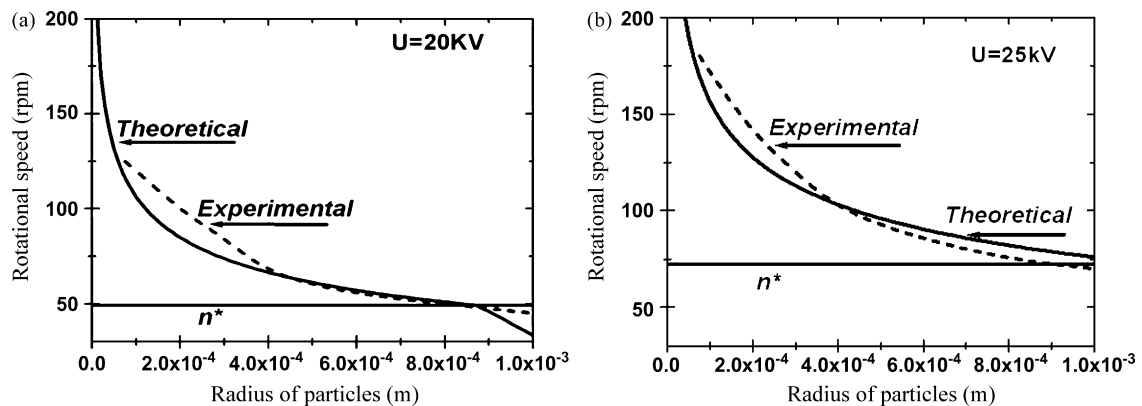


Fig. 8. Experimental relationship curve of critical rotational speed and particle radius: (a) $U = 20$ kV and (b) $U = 25$ kV.

particles get the saturated charging value (Q_s) and adhere on the surface of rotating roll electrode.

From above discussion, the purity and recycle percentages were not simultaneous improved. For example, when rotational speed was increased, metal particles' recycle percentage increased but purity decreased. To increase the detaching critical rotational speed (n') can settle this problem. Then the method of increasing n' are: (1) increasing the number of corona electrodes, width of corona field and electric field strength to increase the charging critical rotational speed (n^*); (2) under the premise of avoiding spark discharge, increasing applied voltage and decreasing discharge gap to increase corona electric field strength and charging value of particles; and (3) changing the curvature of rotating roll electrode and position of corona electrodes to decrease the loss of charge value on the surface of rotating roll electrode. A quantitative method for analyzing the affection of rotational speed was studied in this paper. The deduced equations are applicable for general flat nonmetal particles. This method can be used in waste treatment and industrial mineral separation.

5. Conclusions

- (1) A quantitative method for analyzing the affection of rotational speed was established.
- (2) The judgment equation of charging critical rotational speed (n^*) was deduced: $n^* = (q_s k e) / (40 \pi \epsilon_0 \epsilon_r R)$
- (3) The judgment equation of critical rotational speed of rotating roll electrode (N) was deduced:
 - (i) $n = n' \leq n^*$, $N = n' = \left(\frac{BC}{mR} - \frac{g}{R} \right)^{1/2} \frac{30}{\pi}$;
 - (ii) $n = n' > n^*$, $N = \left(\frac{BC(n^*)^2}{BC - mg} - \frac{g}{R} \left(\frac{30}{\pi} \right)^2 \right)^{1/2}$;
$$B = \frac{9k_1 \pi \epsilon_0 \epsilon_r^2 E_0^2}{(\epsilon_r + 2)^2}, \quad C = \frac{(r^2 + 2rh)^2}{4h^2}.$$
- (4) Analyze the relationship between critical rotational speed and radius of particles. The purity and recycle percentage of materials got a good level when the rotational speed was about 70 rpm. The experimental results have a good agreement with theoretical computed results.

Acknowledgments

This project was supported by the National High Technology Research and Development Program of China (863 program

2006AA06Z364), Program for New Century Excellent Talents in University and the Research Fund for the Doctoral Program of Higher Education (200060248058).

References

- [1] L. Theo., Integrated recycling of non-ferrous metal at Boliden Ltd. IEEE international symposium on Electronics and The Environment, 1998, pp. 42–47.
- [2] L. Dascalescu, A. Samuila, A. Mihalciou, S. Bente, A. Tilmatine, Robust design of electrostatic separation processes, IEEE Trans. Industry Appl. 41 (3) (2005) 715–719.
- [3] F.S. Knoll, J.E. Lawver, J.B. Taylor, Electrostatic separation, in: Ullmann's Encyclopedia of Industrial Chemistry, fifth ed., VCH, Weinheim, 1988, B2: pp. 20-1–20-11.
- [4] R. Morar, R. Munteanu, E. Simion, I. Munteanu, L. Dascalescu, Electrostatic treatment of bean seeds, IEEE Trans. Industry Appl. 35 (1) (1999) 208–212.
- [5] A. Iuga, R. Morar, A. Samuila, L. Dascalescu, Electrostatic separation of metals and plastics from granular industrial wastes, IEE Proc.: Sci., Meas. Technol. 148 (2) (2001) 47–54.
- [6] S. Zhang, E. Forsberg, Optimization of electrodynamic separation for metals recovery from electronic scrap, Conserv. Recycling 22 (1998) 143–162.
- [7] H.M. Veit, T.R. Diehl, A.P. Salami, J.S. Rodrigues, A.M. Bernardes, J.A.S. Tenorio, Utilization of magnetic and electrostatic separation in the recycling of printed circuit boards scrap, Waste Manage. 25 (2005) 67–74.
- [8] J. Li, H. Lu, J. Guo, Z. Xu, Y. Zhou, Recycle technology for recovering resources and products from waste printed circuit boards, Environ. Sci. Technol. 41 (2007) 1995–2000.
- [9] A. Samuila, A. Iuga, R. Morar, R. Tobazeon, L. Dascalescu, Factors which affect the corona charging of insulating spheres on plate and roll electrodes, J. Electrostatic 40–41 (1997) 377–382.
- [10] L. Dascalescu, A. Samuila, A. Iuga, R. Morar, I. Csorvasy, Influence of material superficial moisture on insulation-metal electroseparation, IEEE Trans. Industry Appl. 30 (4) (1994) 844–849.
- [11] L. Dascalescu, R. Tobazeon, P. Atten, Behaviour of conductive particles in corona-dominated electric fields, Industry Applications Society Annual Meeting, vol. 2, 1992, pp. 1479–1486.
- [12] L. Dascalescu, R. Tobazeon, P. Atten, Behaviour of conducting particles in corona-dominated electric fields, J. Phys. D: Appl. Phys. 28 (1995) 1611–1618.
- [13] L. Dascalescu, R. Morar, A. Iuga, A. Samuila, V. Neamtu, I. Suarasan, Charging of particulates in the corona field of roll-type electroseparators, J. Phys. D: Appl. Phys. 27 (1994) 1242–1251.
- [14] Y. Wu, G.S.P. Castle, I.I. Inculet, S. Petigny, G. Swei, Induction charge on freely levitating particles, Powder Technol. 135–136 (2003) 59–64.
- [15] J. Li, H. Lu, Z. Xu, Y. Zhou, A model for computing the trajectories of the conducting particles from waste printed circuit boards in corona electrostatic separators, J. Hazard. Mater. (in press).
- [16] V. Jaiswal, M.J. Thomas, Finite element modelling of ionized field quantities around a monopolar HVDC transmission line, J. Phys. D: Appl. Phys. 36 (2003) 3089–3094.